Diagnostic and prognostic value of CD44v9 and TIM3 expression in CK$^-$ and CK$^+$ regions in gastric cancer tissues

XIAOFEI WANG[1*], LIN LU[2-4*], RUIDONG YANG[5*], ZHIWU WANG[6], QINGKE LI[7], JINGWU LI[4] and YANKUN LIU[2-4]

[1]School of Clinical Medicine, North China University of Science and Technology, Tangshan, Hebei 063200, P.R. China; [2]Department of Medical Molecular Diagnosis, Tangshan People's Hospital, Tangshan, Hebei 063001, P.R. China; [3]Tangshan Key Laboratory of Precision Medicine Testing, Tangshan People's Hospital, Tangshan, Hebei 063001, P.R. China; [4]Hebei Province Key Laboratory of Molecular Oncology, Tangshan People's Hospital, Tangshan, Hebei 063001, P.R. China; [5]Department of Pathology, Luanzhou City People's Hospital, Tangshan, Hebei 063004, P.R. China; [6]Second Department of Radiotherapy and Chemotherapy, Tangshan People's Hospital, Tangshan, Hebei 063001, P.R. China; [7]Department of Gastrointestinal Surgery, Tangshan People's Hospital, Tangshan, Hebei 063001, P.R. China

Received February 18, 2024; Accepted July 15, 2024

DOI: 10.3892/ol.2024.14612

Abstract. The specificity and sensitivity of the current diagnostic and prognostic biomarkers for gastric cancer (GC) are limited. The present study aimed to evaluate the diagnostic and prognostic significance of cluster-of-differentiation gene 44 variant isoform 9 (CD44v9) and T cell immunoglobulin and mucin domain-containing protein 3 (TIM3) expression levels alone or combined in the tumor tissues of patients with GC and reveal the roles of CD44v9 and TIM3 in the cytokeratin (CK)$^+$ and CK$^-$ regions. Multiplex immunofluorescence staining was performed for CD44v9, TIM3 and CK using a tissue microarray. The tissues were divided into three regions based on CK expression: Total, CK$^+$, and CK$^-$ regions. The diagnostic and prognostic value was evaluated using receiver operating characteristic curves, Kaplan-Meier and Cox regression analyses. The results demonstrated that the density of cells expressing CD44v9, TIM3 and co-expressing CD44v9 and TIM3 (CD44v9/TIM3) in both the CK$^+$ and CK$^-$ regions of tumor tissues was significantly higher than those in normal tissues (P<0.001). Moreover, the expression of CD44v9 in the CK$^-$ region was significantly positively correlated with age and tumor grade (P<0.05), and the expression of CD44v9/TIM3 in the CK$^-$ region of tumor tissues was significantly positively correlated with age, tumor grade and metastasis (P<0.05). Furthermore, the area under the curve for TIM3 expression in the CK$^+$ region was 0.709, with a sensitivity of 45.83% and a specificity of 85.54% (P<0.001). High expression of CD44v9 in the CK$^-$ region was also significantly associated with poor survival and independently predicted a poor prognosis in patients with GC (hazard ratio, 2.387; 95% confidence interval, 1.384-4.118; P<0.01). In conclusion, dividing tissue regions based on CK expression is important for the diagnosis of GC. The expression of TIM3 in the CK$^+$ region demonstrated diagnostic potential for GC, and high expression of CD44v9 in the CK$^-$ region was an independent prognostic risk factor for patients with GC.

Correspondence to: Professor Jingwu Li, Hebei Province Key Laboratory of Molecular Oncology, Tangshan People's Hospital, 65 Sheng-Li Road, Tangshan, Hebei 063001, P.R. China
E-mail: tslijingwu@163.com

Dr Yankun Liu, Department of Medical Molecular Diagnosis, Tangshan People's Hospital, 65 Sheng-Li Road, Tangshan, Hebei 063001, P.R. China
E-mail: rmyy_lyk@163.com

*Contributed equally

Key words: gastric cancer, cluster-of-differentiation gene 44 variant isoform 9, T cell immunoglobulin and mucin domain-containing protein 3, diagnostic marker, prognostic marker

Introduction

Gastric cancer (GC) is a common type of digestive system tumor worldwide; specifically, it was the fourth most common cancer worldwide in 2020. Although the mortality rate of GC has declined in certain countries in recent years, it still ranks fifth among cancers worldwide (1,2). At present, biomarkers for the diagnosis and prognosis of GC are derived from serological and tissue specimens, with serum markers such as carcinoembryonic antigen (CEA), carbohydrate antigen (CA)19-9 and CA 72-4 have been used for auxiliary diagnosis and monitoring of GC. However, the optimal treatment window is often missed due to the low specificity and sensitivity of these markers (3). Histological markers, such as Ki67, p27 and p53, also have problems of low sensitivity and specificity for GC diagnosis. Therefore, as pathology is considered the gold standard for cancer diagnosis (4), the present study aimed to explore novel histological biomarkers for the diagnosis and prognosis evaluation of GC.

Cluster-of-differentiation gene 44 (CD44), a cell surface adhesion molecule, has been recognized as a cancer stem

cell marker for several types of cancer, including GC (5). CD44 variant isoform 9 (CD44v9), one of the major protein splice variant isoforms, is highly expressed in human GC tissues (6,7) and has been indicated to be associated with a poor prognosis (8-10). Studies have reported that CD44v9 expression is associated with the pathological features of GC, lung adenocarcinoma, urothelial cancer and bladder cancer (10-13); however, certain studies which focused on the expression of CD44v9 in GC tissues reported inconsistencies in terms of the distribution of patient sex, tumor size, tumor stage and tumor classification strategies (9,10,14). In addition, CD44 is expressed in lymphocytes and macrophages surrounding tumor cells (15,16), but little is known about CD44v9 expression in these cells.

T cell immunoglobulin and mucin domain-containing protein 3 (TIM3), a crucial immune checkpoint protein, is expressed mainly by immune cells, such as T helper cell 1 lymphocytes, cytotoxic lymphocytes, monocytes, macrophages, natural killer (NK) cells and dendritic cells, and is expressed at low levels in tumor cells (17-19). Nevertheless, TIM3 in cancer cells has been considered as an emerging target for GC treatment (20). Recent studies have reached different conclusions regarding the role of tumor-infiltrating $TIM3^+$ cells in predicting the overall survival (OS) of patients with GC (20,21). Given that the CD44 and TIM3 proteins are both expressed in lymphocytes and macrophages, we hypothesized that synchronous expression of CD44v9 and TIM3 in tumor or stromal cells could provide a promising marker for the diagnosis and prognosis evaluation of GC.

In the present study, multiplex immunofluorescence (mIF) was used to detect the expression of CD44v9 and TIM3 in GC tissues. This method can be used to analyze the expression of CD44v9 and TIM3 alone or combined, as well as their expression in cytokeratin $(CK)^+$ and CK^- regions in GC tissues. In addition, the present study assessed the potential clinical value of these proteins in GC diagnosis and prognosis evaluation.

Materials and methods

Study design. mIF was performed to detect the expression of CD44v9 and TIM3 in the CK^+ and CK^- regions of tissues from patients with GC. A total of 96 patients who underwent gastric resection without preoperative therapy between April and November 2009 were included in the present study. The information on the clinicopathological characteristics of the patients and the corresponding tumor tissue microarray (TMA), which contained 180 cores, including 96 tumor tissue cores and 84 matched tumor-adjacent normal tissues cores, was purchased solely from Shanghai Outdo Biotech Co., Ltd. (catalog no. HStmA180Su13). Matched tumor-adjacent normal tissues were unavailable for 12 of the patients. The clinicopathological stage was based on the seventh edition of the American Joint Committee on Cancer Staging Manual (22). The present study was performed with the approval of the Institutional Ethics Committee of the Tangshan People's Hospital (Tangshan, China). Written informed consent was obtained from all patients prior to the study.

TMA preparation. Formalin-fixed, paraffin-embedded (FFPE) GC tissues were evaluated by pathologists. Cores were cut from representative tumor regions and arranged regularly in a blank paraffin block. The tissue cores were then allowed to fuse in a thermostatic oven at 52˚C. Subsequently, the tissue array block was continuously sliced to make a TMA (gastric cancer TMA; cat. no. HStmA180Su13; Shanghai Outdo Biotech Co., Ltd.), which was heated in an oven at 60˚C for 16 h to fix the tissue on the slide. Each core was 1.5 mm in diameter and 4 μm in thickness. Finally, pathologists checked the quality of each core under the Nikon Eclipse E600 light microscope and recorded the diagnosis based on hematoxylin and eosin (H&E) staining. The H&E staining was performed using a fully automatic dyeing machine (Leica ST5020; Leica Microsystems GmbH). The H&E staining process was performed at room temperature. The TMA was treated with xylene I and xylene II separately for 10 min, followed by hydration in 100-70% ethanol for 5 min and rinsing in running water for 1 min. The TMA was placed in hematoxylin staining solution for 5 min, rinsed with running water for 2 min, washed with 1% HCl and PBS buffer, and immersed in water for counterstaining. The TMA was then placed in eosin staining solution for 5 min. Subsequently, the TMA was dehydrated sequentially in 75-100% ethanol, followed by immersion in xylene I and xylene II to complete the staining process.

mIF. The TMA was heated in an oven at 63˚C for 1 h to prepare for dewaxing. Dewaxing and hydration were then performed using a fully automatic dyeing machine (Leica ST5020; Leica Microsystems, Inc.) using xylene and gradient alcohol solution. The TMA was then boiled in 1X repair solution (10X AR6 buffer; cat. no. AR6001KT; Akoya Biosciences, Inc.) for 3 min, heated in a microwave on low power for 15-20 min and cooled at room temperature to complete antigen retrieval. The TMA was then treated with H_2O_2 for 10 min to remove endogenous peroxidase and washed with TBST (0.1% Tween20). The sections were subsequently incubated with blocking buffer (1X Antibody Diluent/Block; cat. no. ARD1001EA; Akoya Biosciences, Inc.) at room temperature for 10 min, primary antibodies at room temperature for 1 h and HRP-conjugated secondary antibodies (EnVision™ FLEX+, Mouse; catalog. no. K8002; and EnVision™ FLEX+, Rabbit; catalog. no. K8009; both Agilent Technologies, Ltd.) at a 1:1 dilution at room temperature for 10 min. After staining with Opal dye at a 1:100 dilution (Opal 7-colour Manual IHC Kit, catalog. no. NEL801001KT; PerkinElmer, Inc.) and incubating at room temperature for 10 min, the TMA was boiled in 1X repair solution (10X AR6 buffer; cat. no. AR6001KT; Akoya Biosciences, Inc.) for 3 min, heated in a microwave on low power for 15-20 min and cooled at room temperature to remove the primary and secondary antibodies (the procedure was consistent with antigen retrieval). The TMA was then washed with TBST (0.1% Tween20). Blocking, incubation with primary antibody, incubation with secondary antibody, Opal staining, and removal of primary and secondary antibodies was repeated until all antibody staining was completed. Detailed information for the primary antibodies is summarized in Table SI. The TMA was counterstained with DAPI (D9542; Sigma-Aldrich; Merck KGaA) at room temperature for 5 min, washed with TBST (0.1% Tween20) and sealed with 1X antifluorescence quenching agent (VECTASHIELD® HardSet™ Antifade Mounting Medium; catalog. no. H-1400; Vector Labs, Inc.).

Multispectral imaging and cell recognition. The TMA-stained images were captured using the TissueFAXS Spectra Systems (TissueGnostics GmbH), which identifies CK^+ cells as tumor cells and CK^- cells as stromal cells in tumor tissue cores. The spectral characteristics of each fluorophore were determined using single-antigen staining, spectrograms were obtained using multispectral fluorescence microscopy, and the signal was identified using StrataQuest analysis software (version 7.1.129; TissueGnostics GmbH). Positive cells were identified according to the intensity and area of the nucleus and antibodies. The cells were divided into CK^+ and CK^- cells. In tumor-adjacent normal tissues cores, CK^+ cells are recognized as normal epithelial cells, whilst CK^- cells are identified as stromal cells (21,23-26). Protein expression was assessed based on the density of cells (number of positive cells/mm^2).

Statistical analysis. Non-normally distributed continuous variables are expressed as the median (lower quartile, upper quartile). The difference in protein expression in tissues was determined using the Mann-Whitney U test and the comparison of protein expression differences among tumor grades was performed using the Kruskal-Wallis H test, followed by a post-hoc Steel-Dwass test. OS rates were assessed using Kaplan-Meier analysis, and the log-rank test was used to plot survival curves. The Cox proportional hazards regression model was used to perform univariate and multivariate survival analyses. Clinical associations were analyzed using the χ^2 test and correlations using Spearman's correlation analysis. Receiver operating characteristic (ROC) curve analysis was used to evaluate the diagnostic value of protein expression for GC and to calculate the cut-off value. $P<0.05$ was considered to indicate a statistically significant difference. The P-value is indicative of a two-sided test. $P<0.01$ and $P<0.001$ were considered to indicate strong significance. All the analyses were performed using SPSS 22.0 (IBM Corp.) and JMP Pro 17.0 (SAS Corp.) statistical software.

Results

Clinical specimens and clinical characteristics. Human tissue samples were collected from 96 patients with GC who had not received chemotherapy or radiotherapy prior to radical resection. Among the 96 tumor tissues and 84 matched tumor-adjacent normal tissues collected for use in the TMA (Fig. S1), the normal tissue of one patient was not included in the analysis due to the absence of epithelial cells. The follow-up period ranged from 5.7 to 6.2 years. As of July 2015, 57/96 patients with GC had died. The mean age of the patients was 64 years. Most of the tumors were concentrated in the gastric antrum (n=50), stomach body (n=25), and cardia (n=8). There was 13 cases of GC involving two or more than two sites of the stomach. The pathological types of the patients with GC included adenocarcinoma (n=76), signet ring cell carcinoma (n=12), mucinous cell carcinoma (n=7) and undifferentiated carcinoma (n=1). The clinical characteristics of the patients with GC are presented in Table I.

Table I. Clinical characteristics of patients with gastric cancer (n=96).

Characteristic	n (%)
Sex	
Male	65 (67.7)
Female	31 (32.3)
Age, years	
<65	51 (53.1)
≥65	45 (46.9)
Tumor size, cm	
≤5	49 (51.0)
>5	47 (49.0)
T classification	
T1	2 (2.1)
T2	11 (11.5)
T3	50 (52.1)
T4	33 (34.4)
N classification	
N0	20 (20.8)
N1	19 (19.8)
N2	25 (26.0)
N3	32 (33.3)
M classification	
M0	94 (97.9)
M1	2 (2.1)
TNM stage	
I	8 (8.3)
II	27 (28.1)
III	59 (61.5)
IV	2 (2.1)
Pathological grade	
G2	16 (16.7)
G3	73 (76.0)
G4	7 (7.3)

T, tumor; N, node; M, metastasis; G, grade.

Expression of CD44v9 and TIM3 and their co-expression in the CK^+ and CK^- regions of tumor tissues and adjacent normal tissues from patients with GC. The expression levels of CD44v9, TIM3 and CK were assessed using mIF staining. CK was used as a marker to distinguish tumor cells from stromal cells. Tumor cells were predominantly present in the CK^+ regions, and stromal cells were present in the CK^- region (Fig. 1A). An ideograph of the CK^+ and CK^- regions in GC tissues and normal gastric tissues is presented in Fig. 1B. First, the differences in CD44v9 and TIM3 expression between tumor tissues and adjacent normal tissues of patients with GC were evaluated. There was no significant difference in CD44v9 expression (P=0.05; Fig. 1C). However, the density of cells expressing TIM3 and co-expressing CD44v9 and TIM3 (CD44v9/TIM3) was significantly greater in tumor tissues than in normal tissues ($P<0.001$; Fig. 1D and E). Second, differences in the density of cells expressing CD44v9, TIM3 and CD44v9/TIM3 between the CK^+ and CK^- regions of the tumor tissues were assessed. It was demonstrated that the density

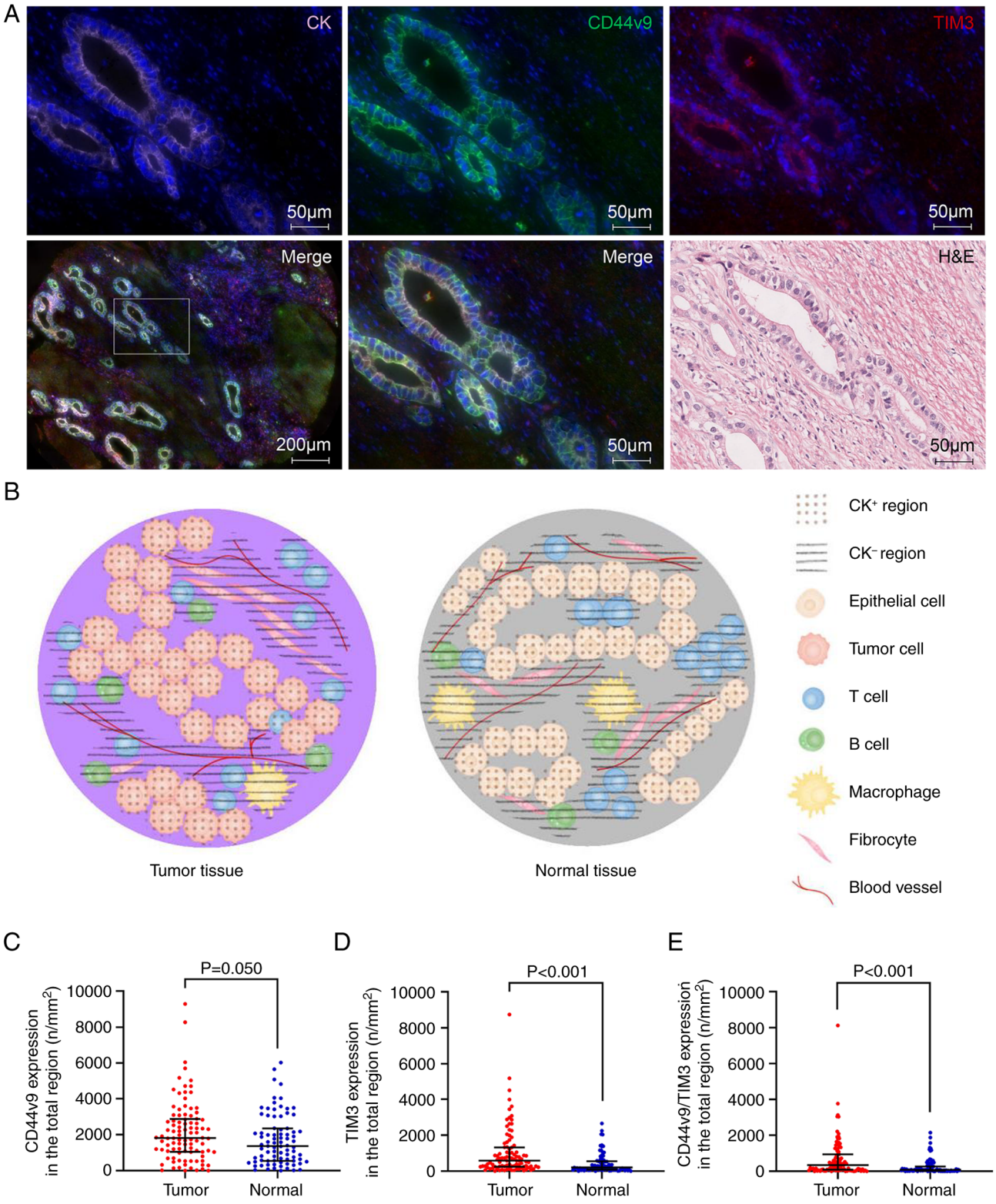

Figure 1. Protein expression of CD44v9 and TIM3 in gastric cancer tissues. (A) Multiplex immunofluorescence and hematoxylin and eosin staining profiles of tumor tissues (DAPI, blue; CK, pink; CD44v9, green; and TIM3, red). (B) Tissue segmentation. Density of (C) CD44v9$^+$, (D) TIM3$^+$ and (E) CD44v9$^+$/TIM3$^+$ cells in tumor and normal tissues. CD44v9, cluster-of-differentiation gene 44 variant isoform 9; TIM3, T cell immunoglobulin and mucin domain-containing protein 3; CK, cytokeratin.

of cells expressing CD44v9, TIM3 and CD44v9/TIM3 was significantly higher in the CK$^+$ region than in the CK$^-$ region (P<0.001; Table II). Finally, the differences in the density of cells expressing CD44v9, TIM3 and CD44v9/TIM3 in the CK$^+$ region or the CK$^-$ region between the tumor tissues and normal tissues was assessed. It was demonstrated that the density of cells with these three expression patterns was significantly higher in the CK$^+$ and CK$^-$ regions of tumor tissues than in normal tissues (P<0.05; Table III). Among the CD44v9$^+$ cells, 16.67, 17.15 and 15.78% were dual-positive cells (the cells

Table II. Comparison of the density of cells expressing multiplex immunofluorescence markers in cytokeratin-positive and -negative regions of gastric cancer tissues.

mIF marker	CK^+ region, n/mm^2	CK^- region, n/mm^2	P-value
CD44v9	5,413.08 (2,944.84, 7,726.14)	952.08 (408.96, 1,617.90)	<0.001[a]
TIM3	854.27 (267.89, 2861.04)	401.74 (160.16, 958.02)	<0.001[a]
CD44v9/TIM3	802.60 (200.58, 2423.22)	156.93 (25.80, 431.16)	<0.001[a]

[a]P<0.05. Data were analyzed using the Mann-Whiney U test, and are presented as median (lower quartile, upper quartile). mIF, multiplex immunofluorescence; CD44v9, cluster-of-differentiation gene 44 variant isoform 9; TIM3, T cell immunoglobulin and mucin domain-containing protein 3; CK, cytokeratin.

Table III. Comparison of the density of cells expressing multiplex immunofluorescence markers in gastric cancer and normal tissues of different regions.

A, CK^+ region

mIF marker	Cancer tissue, n/mm^2	Normal tissue, n/mm^2	P-value
CD44v9	5,413.08 (2,944.84, 7726.14)	3,162.35 (1,837.03, 4731.01)	<0.001[a]
TIM3	854.27 (267.89, 2861.04)	214.37 (57.40, 823.47)	<0.001[a]
CD44v9/TIM3	802.60 (200.58, 2423.22)	177.38 (37.03, 705.24)	<0.001[a]

B, CK^- region

CD44v9	952.08 (408.96, 1617.90)	502.40 (180.41, 1292.61)	0.016[a]
TIM3	401.74 (160.16, 958.02)	186.88 (76.22, 420.92)	<0.001[a]
CD44v9/TIM3	156.93 (25.80, 431.16)	33.03 (6.74, 143.50)	<0.001[a]

[a]P<0.05. Data were analyzed using the Mann-Whiney U test, and are presented as median (lower quartile, upper quartile). mIF, multiplex immunofluorescence; CD44v9, cluster-of-differentiation gene 44 variant isoform 9; TIM3, T cell immunoglobulin and mucin domain-containing protein 3; CK, cytokeratin.

co-expressing CD44v9 and TIM3) in the total, CK^+ and CK^- regions, respectively, of the tumor tissues. However, among the $TIM3^+$ cells, 27.09, 92.57 and 37.28% were dual-positive cells in the total, CK^+ and CK^- regions, respectively, of the tumor tissues. These data indicate that the expression levels of CD44v9, TIM3 and CD44v9/TIM3 were higher in the CK^+ regions compared with in the CK^- regions in tumor tissues, and overall, the expression levels in tumor tissues were higher than in normal tissues.

Correlations between clinical characteristics and the expression of CD44v9 and TIM3, and their co-expression in the CK^+ and CK^- regions of tumor tissues from patients with GC. To assess the potential value of CD44v9 and TIM3 in the diagnosis of GC, the present study analyzed the correlations between the density of cells expressing CD44v9, TIM3 and CD44v9/TIM3 in the CK^+ and CK^- regions of tumor tissues and pathological features. It was revealed that the density of cells positive for CD44v9, TIM3 and CD44v9/TIM3 in the total, CK^+ and CK^- regions was significantly positively correlated with patient age (P<0.05; Tables IV, SII and SIII). Additionally, the density of cells expressing CD44v9 in the CK^- region was positively correlated with tumor grade (P<0.01; Table IV), and the density of cells expressing CD44v9 in the CK^- region was significantly higher in grade (G)4 GC samples than in G2 and G3 GC samples (P<0.05; Fig. 2A). Similarly, the density of cells expressing CD44v9/TIM3 in the CK^- region of tumor tissues was significantly positively correlated with tumor grade and metastasis (P<0.05; Table IV), and the density of cells expressing CD44v9/TIM3 in the CK^- region was significantly higher in G4 GC samples than in G3 samples (P<0.05; Fig. 2B). The ROC curves based on CD44v9, TIM3 and CD44v9/TIM3 expression patterns in different regions are presented in Figs. 2C and S2. The expression of CD44v9 in the total region of cancer tissues was not significant for diagnosis of GC (P=0.050), whereas its expression was significant for GC diagnosis when distinguishing CK^+ (P<0.016) and CK^- (P=0.016) regions. TIM3 in the CK^+ region had the largest area under the curve (AUC) and the highest diagnostic specificity (85.54%). Moreover, TIM3 also showed the highest diagnostic sensitivity (71.88%) in the total region (Table V). The AUC of CD44v9 and TIM3 and the CD44v9/TIM3 was higher in CK^+ regions than in the total region and CK^- region (Table V; Figs. 2C and S2). These results indicate that the expression of

Table IV. Correlation between clinical characteristics and the expression of multiplex immunofluorescence markers in the cytokeratin-negative region in patients with gastric cancer (n=96).

	CD44v9		TIM3		CD44v9/TIM3	
Characteristic	r_s	P-value	r_s	P-value	r_s	P-value
Sex	0.180	0.080	0.152	0.141	0.127	0.216
Age	0.245	0.016[a]	0.203	0.047[a]	0.235	0.021[a]
Tumor size	0.018	0.863	0.060	0.561	0.045	0.663
T classification	-0.096	0.350	-0.057	0.582	-0.065	0.526
N classification	0.060	0.563	0.143	0.164	0.135	0.190
M classification	0.176	0.086	0.192	0.061	0.208	0.042[a]
TNM stage	-0.023	0.826	0.055	0.596	0.041	0.690
Pathological grade	0.272	0.007[a]	0.197	0.054	0.202	0.049[a]

[a]P<0.05. r_s, Spearman's rank correlation coefficient; mIF, multiplex immunofluorescence; CD44v9, cluster-of-differentiation gene 44 variant isoform 9; TIM3, T cell immunoglobulin and mucin domain-containing protein 3; T, tumor; N, node; M, metastasis.

Table V. Receiver operating characteristic curve analysis of gastric cancer for the expression of multiplex immunofluorescence markers in different regions.

Index	AUC	P-value	Cut-off, n/mm^2	Sensitivity, %	Specificity, %
Total					
CD44v9	0.585	0.050	1,035.81	77.08	40.96
TIM3	0.690	<0.001[a]	261.08	71.88	60.24
CD44v9/TIM3	0.680	<0.001[a]	613.59	62.50	69.88
CK+					
CD44v9	0.704	<0.001[a]	3,922.86	67.71	69.88
TIM3	0.709	<0.001[a]	1,225.51	45.83	85.54
CD44v9/TIM3	0.703	<0.001[a]	750.57	52.08	81.93
CK-					
CD44v9	0.604	0.016[a]	512.57	68.75	53.01
TIM3	0.665	<0.001[a]	320.76	57.29	71.08
CD44v9/TIM3	0.688	<0.001[a]	63.65	67.71	66.27

[a]P<0.05. AUC, area under the curve; CD44v9, cluster-of-differentiation gene 44 variant isoform 9; TIM3, T cell immunoglobulin and mucin domain-containing protein 3; CK, cytokeratin.

CD44v9 and TIM3 in accurate regions based on CK- and CK+ could provide higher diagnostic value for GC.

Prognostic value of the expression of CD44v9 and TIM3 and their co-expression in the CK+ and CK- regions of tumor tissues from patients with GC. To analyze the prognostic value of CD44v9, TIM3 and CD44v9/TIM3 expression in the CK+ and CK- regions of tumor tissues, the patients with GC were divided into a high- and low-expression group according to the median density of cells expressing the indicator proteins. The differences between the high- and low-expression groups were then compared. The results demonstrated that the 5-year survival rates of patients with high and low CD44v9 expression in the CK- region were 31.25 and 68.75%, respectively. The OS of patients with GC with high CD44v9 expression in the CK- region was significantly shorter than that of patients with low CD44v9 expression (P<0.01; Fig. 3C and D). This indicates that a high expression of CD44v9 in the CK- region predicts a poor prognosis in patients with GC. However, the survival curves did not significantly differ between patients with GC with high or low expression of other markers (P<0.05; Figs. 3A and B, and S3). Furthermore, univariate analysis of the markers and pathological features demonstrated that tumor (T) classification, node (N) classification, metastasis (M) classification, TNM stage, and the expression of CD44v9 in the CK- region, were significant factors influencing OS in patients with GC. Multivariate analysis indicated that high expression of CD44v9 in the CK- region was a significant independent risk factor predicting the OS of patients with GC (P<0.01; hazard ratio, 2.387; 95% confidence interval, 1.384-4.118; Table VI). Taken together, these findings indicate

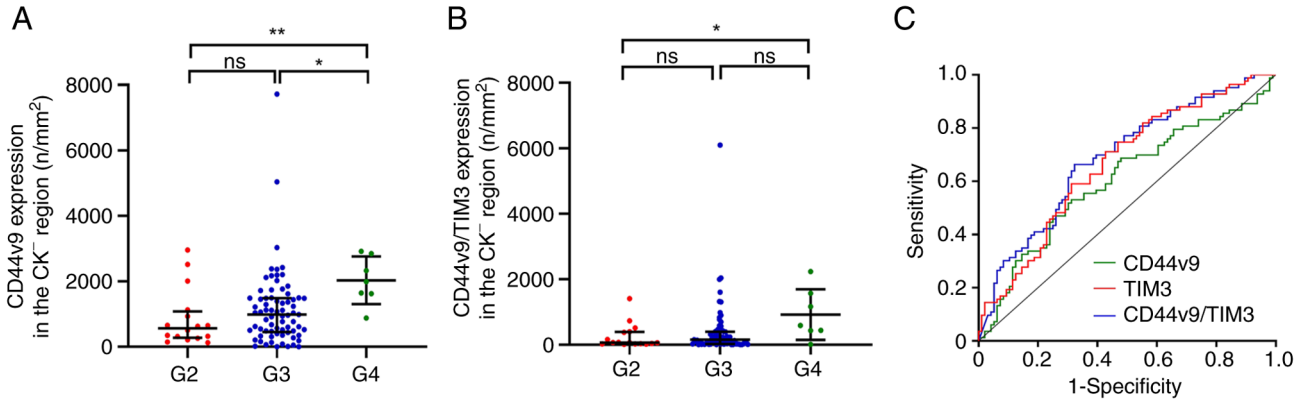

Figure 2. Association between CD44v9 expression in the CK- region of tumor tissues and tumor grade. Density of (A) CD44v9+ and (B) CD44v9/TIM3+ cells in the CK- region in G2, G3 and G4 gastric cancer tissues. (C) Receiver operating characteristic curves of the density of CD44v9+, TIM3+ and CD44v9+/TIM3+ cells in the CK- region of tumor tissues for the diagnosis of gastric cancer. *P<0.05 and **P<0.01. ns, not significant; CD44v9, cluster-of-differentiation gene 44 variant isoform 9; TIM3, T cell immunoglobulin and mucin domain-containing protein 3; CK, cytokeratin; G, grade.

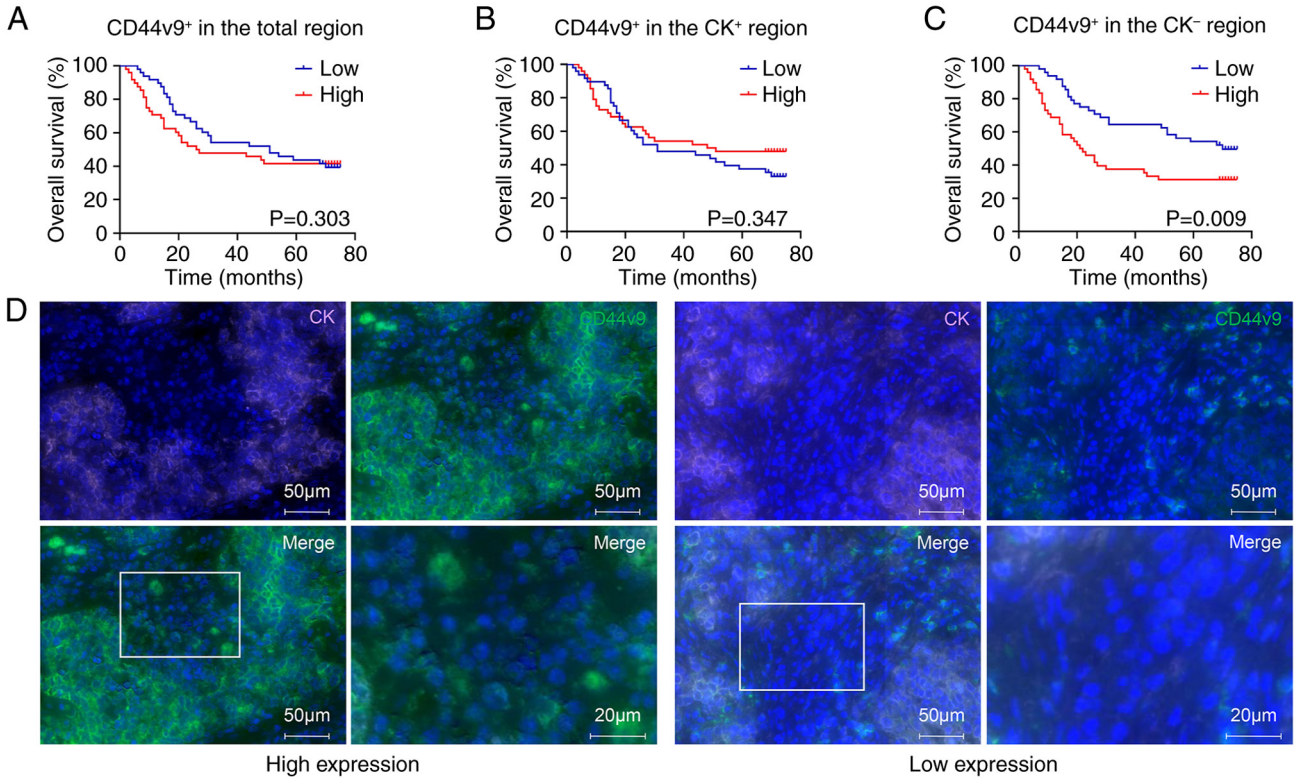

Figure 3. Overall survival of patients with gastric cancer with high and low CD44v9 expression in tumor tissues. Kaplan-Meier plots of overall survival in the (A) total, (B) CK+ and (C) CK- regions of tumor tissues. (D) Representative images of gastric cancer cells with high and low expression of CD44v9 in the CK- region (DAPI, blue; CK, pink; CD44v9, green). CD44v9, cluster-of-differentiation gene 44 variant isoform 9; TIM3, T cell immunoglobulin and mucin domain-containing protein 3; CK, cytokeratin.

that the expression of CD44v9 in the CK- region could be of great prognostic value for patients with GC.

Discussion

The tumor microenvironment (TME) has been reported to serve crucial roles in the development, differentiation, survival and proliferation of cancer cells (27,28). In addition to tumor cells, fibroblasts, immune cells (such as T lymphocytes, B lymphocytes, NK T cells and tumor-associated macrophages) and stromal cells (such as pericytes and certain adipocytes) are involved in the TME (28). In the past, studies on biomarkers in cancer tissues have focused on tumor cells in tumor tissues, ignoring stromal cells. However, certain biomarkers, such as TIM3, are expressed in both tumor cells and stromal cells (18). Therefore, the present study aimed to assess the expression of CD44v9 and TIM3 and the co-expression of CD44v9 and TIM3 in tumor cells and stromal cells using mIF to evaluate the potential clinical value of these biomarkers for the evaluation if the diagnosis and prognosis of GC.

Table VI. Cox univariate multivariate regression for overall survival in patients with gastric cancer.

	Univariate Cox		Multivariate Cox	
Variable	HR (95% CI)	P-value	HR (95% CI)	P-value
Sex (female vs. male)	1.109 (0.639-1.923)	0.714		
Age (≥65 vs. <65 years)	1.379 (0.820-2.318)	0.226		
Tumor size (>5 vs. ≤5 cm)	1.648 (0.976-2.785)	0.062		
Tumor grade (G4 vs. G2 and G3)	2.025 (0.807-5.085)	0.133		
TNM stage (III and IV vs. I and II)	3.016 (1.592-5.715)	0.001[a]	1.655 (0.747-3.668)	0.215
T classification (T3 and T4 vs. T1 and T2)	4.066 (1.270-13.020)	0.018[a]	2.196 (0.911-10.235)	0.222
N classification (N1, N2 and N3 vs. N0)	5.315 (1.920-14.713)	0.001[a]	3.054 (0.747-3.668)	0.070
M classification (M1 vs. M0)	6.678 (1.576-28.290)	0.010[a]	3.073 (0.708-13.345)	0.134
CD44v9 expression				
In total region (High vs. low)	1.156 (0.687-1.943)	0.585		
In CK^+ region (High vs. low)	0.780 (0.462-1.317)	0.352		
In CK^- region (High vs. low)	1.989 (1.173-3.373)	0.011[a]	2.387 (1.384-4.118)	0.002[a]
TIM3 expression				
In total region (High vs. low)	1.374 (0.816-2.314)	0.231		
In CK^+ region (High vs. low)	1.352 (0.803-2.275)	0.257		
In CK^- region (High vs. low)	1.595 (0.943-2.696)	0.082		
CD44v9/TIM3 expression				
In total region (High vs. low)	1.272 (0.756-2.139)	0.365		
In CK^+ region (High vs. low)	1.423 (0.845-2.397)	0.184		
In CK^- region (High vs. low)	1.539 (0.913-2.594)	0.106		

[a]P<0.05. HR, hazard ratio; CI, confidence interval; CD44v9, cluster-of-differentiation gene 44 variant isoform 9; TIM3, T cell immunoglobulin and mucin domain-containing protein 3; T, tumor; N, node; M, metastasis; G, grade; CK, cytokeratin.

In the present study, the assessment of CD44v9 and TIM3 expression in tissues differs from traditional qualitative and semi-quantitative immunohistochemistry (IHC) methods (29-32). H&E staining and mIF assays were performed, which used an automated pathological imaging system to identify and count the number of positive cells/mm^2. This is a quantitative approach for assessing protein expression levels in tissues and qualified for histopathology of cancer study (21,23-24). Although the scoring system of traditional IHC has been used in many studies to measure protein expression, inconsistent results are common (8,10,14). For example, tissues with low densities of positive cells are recorded as zero (8). Thus, the present study directly adopted the method of measuring the density of positive cells instead of immunofluorescence scores. Furthermore, the cancer cells could be distinguished from stromal cells according to CK expression, not the normal cells. Therefore, the diagnosis of GC was according to the density of cells expressing CD44v9 or TIM3 in the CK^+ region. It was demonstrated that the expression of CD44v9 in the CK^+ region of tumor tissues was greater than that in normal tissues, which indicates that CD44v9 function as an oncogene in GC development. Considering the disruption of the intracellular reactive oxygen species (ROS)/glutathione (GSH) balance (such as excessive ROS production) leading to energy homeostasis imbalance and tumor cell death (33), and the decrease in intracellular ROS casused by CD44v9 via upregulation of cystine uptake and promotion of GSH synthesis in GC cells (34,35), we hypothesize that CD44v9 may promote GC cell proliferation by intracellular decrease of ROS. Moreover, the present study demonstrated that $CD44v9^+$ epithelial cells could be scattered or clustered in normal tissues. Similar studies reported that the CD44v9 expression could occur in the regenerated gastric epithelium cells or gastric epithelium cells infected with *H. pylori* (36-38), as well as the expansion of stem cells of gastric tissues (37).

Nevertheless, a previous study ignored the distinction between the parenchyma and stroma in GC tissues (10). CD44 was previously reported to be expressed in T cells, B cells and macrophages (16,39-41) and it has been reported to be upregulated in M2 macrophages, and the deletion of CD44 hinders the polarization of macrophages, suppressed the migration of tumor cells (41). As a variant subtype of CD44, CD44v9 has been reported to be overexpressed in myeloma plasma cells, which could promote the adhesion of stromal cells and the secretion of IL-6, which promotes cell proliferation, anti-apoptosis, invasion and metastasis through the activation of the JAK/STAT3 signaling pathway (42,43). In addition, CD44v9 could be also expressed in T cells (44). A previous review revealed that ROS can modulate the TME by affecting several stromal cells that provide metabolic support and blood supply, and facilitate immune responses to tumors (45). The T cell-dependent antitumor response is also dependent on

ROS (45). Overexpression of CD44v9 in stromal cells may disrupt the balance of ROS in T cells and affect the antitumor function of T cells. Based on this evidence, we hypothesize that high expression of CD44v9 in stromal cells may promote tumor growth. In the present study, it was demonstrated that the density of $CD44v9^+$ cells in the CK^- region of tumor tissues was greater than that in normal tissues, but lower than that in the CK^+ region. The expression of CD44v9 in the CK^- region of tumor tissues was positively correlated with tumor grade and age. In addition, patients with GC with high CD44v9 expression in the CK^- region experienced a worse OS rate than those with low CD44v9 expression, and CD44v9 was identified as an independent risk factor for GC. The univariate Cox analysis revealed a difference between stages I-II and stages III-IV ($P<0.05$). However, the multivariate Cox analysis did not demonstrate a statistical difference between the two groups. TNM staging was considered to be a potential confounding factor in the statistical analysis, which highlighted the importance of the expression level of CD44v9 in the CK^- region for prognosis of GC. The TNM staging may be a confounding variable that indirectly affected the survival rates, exhibiting a 'false association' with the outcome. Adjusting for confounders in regression allows for the identification of independent contributors to the outcomes (46,47). Additionally, similar studies have also indicated that certain prognostic factors, such as TNM stage and tumor size (21,48,49), do not always hold statistical significance in Cox regression analyses.

TIM3 is an immune checkpoint, and its activation can increase T-cell dysfunction and exhaustion (50). TIM3 has been also recognized to inhibit NK cell activity by binding to phosphatidyl serine (51). The two aforementioned studies reported that overexpression of TIM3 in immune cells could promote tumor cell growth. However, previous studies have reported that TIM3 is mainly expressed in immune cells, and rarely expressed in epithelial-origin tumor cells, such as GC cells and lung adenocarcinoma cells (18,19,52). The present study demonstrated that the expression of TIM3 in tumor tissues was higher than that in normal tissues, which is consistent with the findings of Wang *et al* (18) and Chen *et al* (20). Furthermore, the present study revealed that the expression of TIM3 in the CK^+ region was higher than that in the CK^- region in tumor tissues, contrary to the findings of Wu *et al* (21). Thus, we hypothesize that TIM3 originated from epithelial cells, and the different results based on the same method may be caused by the histological heterogeneity of GC tissue cores or the limited number of cases. The histological heterogeneity includes individual characteristics, GC tissue collection site and the quantity of T cell infiltration (53). Although the CK^+ and CK^- regions were distinguished based on rigorous examination, certain CK^- immune cells were inevitably incorporated into the CK^+ region at the edge of the region, so this analysis method needs to be improved. Moreover, in the present study, the sensitivity of TIM3 in the total region was 71.88%, and the specificity of TIM3 in CK^+ region for diagnosing GC was 85.54%. Previous studies have reported that the sensitivity of Ki67 and p27 for diagnosis in different histological types of GC ranges from 46.3-62.4% (54,55), which are all lower than the sensitivity of the biomarkers in the present study. A previous study also reported that the sensitivity of p53 in intestinal type adenocarcinoma was 83%, and sensitivity for diagnosis of signet ring cell carcinoma was only 69% (56). A previous study showed that soluble TIM3 in the serum of patients with GC could be detected by ELISA, with diagnostic sensitivity (73.98%) and specificity (95.89%) higher than TIM3 in the tissues of the present study (57). However, the sensitivity of TIM3 in tissue specimens in the present study for GC diagnosis is higher than the combined sensitivity of CA 72-4, CA 19-9 and CEA in serum (58). The role of TIM3 in serum and tissue for GC diagnosis should be further researched through comparative studies in future.

In the present study, the AUC for CD44v9/TIM3 in the CK^- region was 0.688, which was higher the AUCs for CD44v9 and TIM3 in the CK^- region alone. Moreover, the density of cells expressing CD44v9/TIM3 was positively correlated with age, M classification and tumor grade. The diagnostic value of CD44v9 combined with TIM3 in the CK^- region was greater than that of each factor individually. This indicates that the combination of CD44v9 and TIM3 provides better clinical significance than either factor alone. However, considering the time-consuming and high cost of mIF, the expression of CK, TIM3 and CD44v9 could be detected by individual or combined staining of the traditional IHC method in clinical application. This traditional IHC requires thorough training for pathologists, which is time-consuming, labor-intensive and requires more tissues for multiple biomarkers. For the TMA used in the present study, multiple biomarkers could be detected in one experiment by using a few tissue samples, and the StrataQuest analysis software could quantitatively analyze different fluorophores, not depending on the subjectivity of pathologists. Although the present study did not use IHC, it is recommended that appropriate testing methods are selected according to the sample size and cost in clinical applications.

The present study has certain limitations: i) The FFPE tissue specimens of patients with GC were preserved for a relatively long time. Although several studies used samples that were preserved for similar amount of time to those in the present study (20,21), the length of time inevitably affected the detection effect of CK, TIM3 and CD44v9; ii) the size of the tissue samples were small, increasing the heterogeneity. It is therefore necessary to recruit recent patients and increase the sample size to reduce limitations in future studies; and iii) the role of CD44v9 in GC diagnosis determined in the present study is based on clinical samples, not *in vitro* and *in vivo* experiments. Thus, we can only hypothesize that CD44v9 acted as an oncogene through ROS on immune responses. Further study on the mechanism of CD44v9 in GC development needs to be researched in the future.

In summary, dividing tissue regions based on CK expression is important for the diagnosis of GC. Moreover, TIM3 in the CK^+ region demonstrated diagnostic potential for GC. High expression of CD44v9 in the CK^- region was an independent risk factor predicting the prognosis of GC. Although CD44v9/TIM3 expression in the CK^- region exhibited lower diagnostic value than TIM3 in the CK^+ region, CD44v9/TIM3 expression in the CK^- region was associated with the degree of GC metastasis and differentiation, highlighting the need for future research.

Acknowledgements

Not applicable.

Funding

The present work was supported by the Natural Science Foundation of Hebei Province (grant no. H2021105019).

Availability of data and materials

The data generated in the present study may be requested from the corresponding author.

Authors' contributions

YL and JL conceived and designed the project. LL and RY collected and sorted the data. XW and LL performed the statistical analysis of the data. RY, ZW and QL analyzed the pathological images. The first draft of the manuscript was written by XW and all authors commented on previous versions of the manuscript. XW and YL confirm the authenticity of all the raw data. All authors have read and approved the final manuscript.

Ethics approval and consent to participate

The present study was performed in line with the principles of the Declaration of Helsinki. Approval was granted by the Ethics Committee of the Tangshan People's Hospital (Tangshan, China; approval no. RMYY-LLKS-2023203). Written informed consent was obtained from all participants included in the present study.

Patient consent for publication

Not applicable.

Competing interests

The authors declare that they have no competing interests.

References

1. Sedeta E, Sung H, Laversanne M, Bray F and Jemal A: Recent mortality patterns and time trends for the major cancers in 47 countries worldwide. Cancer Epidemiol Biomarkers Prev 32: 894-905, 2023.
2. Sung H, Ferlay J, Siegel RL, Laversanne M, Soerjomataram I, Jemal A and Bray F: Global cancer statistics 2020: Globocan estimates of incidence and mortality worldwide for 36 cancers in 185 countries. CA Cancer J Clin 71: 209-249, 2021.
3. Matsuzaki J, Tsugawa H and Suzuki H: Precision medicine approaches to prevent gastric cancer. Gut and Liver 15: 3-12, 2021.
4. Wang FH, Zhang XT, Tang L, Wu Q, Cai MY, Li YF, Qu XJ, Qiu H, Zhang YJ, Ying JE, *et al*: The Chinese society of clinical oncology (CSCO): Clinical guidelines for the diagnosis and treatment of gastric cancer. Cancer Commun (Lond) 44: 127-172, 2023.
5. Morath I, Hartmann TN and Orian-Rousseau V: CD44: More than a mere stem cell marker. Int J Biochem Cell Biol 81: 166-173, 2016.
6. Choi ES, Kim H, Kim HP, Choi Y and Goh SH: CD44v8-10 as a potential theranostic biomarker for targeting disseminated cancer cells in advanced gastric cancer. Sci Rep 7: 4930, 2017.
7. Harn HJ, Ho LI, Chang JY, Wu CW, Jiang SY, Lee HS and Lee WH: Differential expression of the human metastasis adhesion molecule CD44V in normal and carcinomatous stomach mucosa of Chinese subjects. Cancer 75: 1065-71, 1995.
8. Hirata K, Suzuki H, Imaeda H, Matsuzaki J, Tsugawa H, Nagano O, Asakura K, Saya H and Hibi T: CD44 variant 9 expression in primary early gastric cancer as a predictive marker for recurrence. Br J Cancer 109: 379-386, 2013.
9. Go SI, Ko GH, Lee WS, Kim RB, Lee JH, Jeong SH, Lee YJ, Hong SC and Ha WS: CD44 variant 9 serves as a poor prognostic marker in early gastric cancer, but not in advanced gastric cancer. Cancer Res Treat 48: 142-152, 2016.
10. Yamakawa Y, Kusuhara M, Terashima M, Kinugasa Y, Sugino T, Abe M, Mochizuki T, Hatakeyama K, Kami K and Yamaguchi K: CD44 variant 9 expression as a predictor for gastric cancer recurrence: Immunohistochemical and metabolomic analysis of surgically resected tissues. Biomed Res 38: 41-52, 2017.
11. Akamine T, Tagawa T, Ijichi K, Toyokawa G, Takamori S, Hirai F, Okamoto T, Oda Y and Maehara Y: The significance of CD44 variant 9 in resected lung adenocarcinoma: Correlation with pathological early-stage and FGFR mutation. Ann Surg Oncol 26: 1544-1551, 2019.
12. Hagiwara M, Kikuchi E, Tanaka N, Kosaka T, Mikami S, Saya H and Oya M: Variant isoforms of CD44 involves acquisition of chemoresistance to cisplatin and has potential as a novel indicator for identifying a cisplatin-resistant population in urothelial cancer. BMC Cancer 18: 113, 2018.
13. Ogihara K, Kikuchi E, Okazaki S, Hagiwara M, Takeda T, Matsumoto K, Kosaka T, Mikami S, Saya H and Oya M: Sulfasalazine could modulate the CD44v9-xCT system and enhance cisplatin-induced cytotoxic effects in metastatic bladder cancer. Cancer Sci 110: 1431-141, 2019.
14. Jogo T, Oki E, Nakanishi R, Ando K, Nakashima Y, Kimura Y, Saeki H, Oda Y, Maehara Y and Mori M: Expression of CD44 variant 9 induces chemoresistance of gastric cancer by controlling intracellular reactive oxygen spices accumulation. Gastric Cancer 24: 1089-1099, 2021.
15. Zhang Y, Gao J, He Y, Qi Z, Qian L, Chen W, Xu H, Yue Y, Mao X, Guo S, *et al*: Vascular normalization was associated with colorectal tumor regression upon anti-PD-L1 combinational therapy. J Immunology Res 2023: 5867047, 2023.
16. Solier S, Müller S, Cañeque T, Versini A, Mansart A, Sindikubwabo F, Baron L, Emam L, Gestraud P, Pantoș GD, *et al*: A druggable copper-signalling pathway that drives inflammation. Nature 617: 386-394, 2023.
17. He Y, Cao J, Zhao C, Li X, Zhou C and Hirsch FR: TIM-3, a promising target for cancer immunotherapy. Onco Targets Ther 11: 7005-7009, 2018.
18. Wang Y, Zhao E, Zhang Z, Zhao G and Cao H: Association between Tim-3 and Gal-9 expression and gastric cancer prognosis. Oncol Rep 40: 2115-2126, 2018.
19. Qin S, Dong B, Yi M, Chu Q and Wu K: Prognostic values of TIM-3 expression in patients with solid tumors: A meta-analysis and database evaluation. Front Oncol 10: 1288, 2020.
20. Chen K, Gu Y, Cao Y, Fang H, Lv K, Liu X, He X, Wang J, Lin C, Liu H, *et al*: TIM3+ cells in gastric cancer: Clinical correlates and association with immune context. Br J Cancer 126: 100-108, 2021.
21. Wu Y, Chen YQ, Shi TG, Tan NJ and Chen WC: Study of immunophenotypic characteristics, clinicopathological parameters and prognosis in gastric cancer microenvironment. Zhonghua Yi Xue Za Zhi 103: 2786-2794, 2023 (In Chinese).
22. Edge SB, Byrd DR, Compton CC, Fritz AG, Greene FL and Trotti A: AJCC cancer staging manual. Seventh edition. Springer, New York, pp117-126, 2010.
23. Lin L, Li H, Wang X, Wang Z, Su G, Zhou J, Sun S, Ma X, Chen Y, You C, *et al*: Components of the tumor immune microenvironment based on m-IHC correlate with prognosis and subtype of triple-negative breast cancer. Cancer Med 12: 21639-21650, 2023.
24. Zuo WW, Zhao CF, Li Y, Sun HY, Ma GM, Liu YP and Kang S: High expression of PARP1 in tumor and stroma cells predicts different prognosis and platinum resistance in patients with advanced epithelial ovarian cancer. Front Oncol 12: 931445, 2022.
25. Moll R, Divo M and Langbein L: The human keratins: Biology and pathology. Histochem Cell Biol 129: 705-733, 2008.
26. Chu PG and Weiss LM: Keratin expression in human tissues and neoplasms. Histopathology 40: 403-439, 2002.
27. Antonio MJ, Zhang C and Le A: Different tumor microenvironments lead to different metabolic phenotypes. Adv Exp Med Biol 1311: 137-147, 2021.
28. Hui L and Chen Y: Tumor microenvironment: Sanctuary of the devil. Cancer Lett 368: 7-13, 2015.
29. Taube JM, Akturk G, Angelo M, Engle EL, Gnjatic S, Greenbaum S, Greenwald NF, Hedvat CV, Hollmann TJ, Juco J, *et al*: The society for immunotherapy of cancer statement on best practices for multiplex immunohistochemistry (IHC) and immunofluorescence (IF) staining and validation. J Immunother Cancer 8: e000155, 2020.

30. Harms PW, Frankel TL, Moutafi M, Rao A, Rimm DL, Taube JM, Thomas D, Chan MP and Pantanowitz L: Multiplex immunohistochemistry and immunofluorescence: A practical update for pathologists. Mod Pathol 36: 100197, 2023.
31. Stack EC, Wang C, Roman KA and Hoyt CC: Multiplexed immunohistochemistry, imaging, and quantitation: A review, with an assessment of Tyramide signal amplification, multispectral imaging and multiplex analysis. Methods 70: 46-58, 2014.
32. Granier C, Vinatier E, Colin E, Mandavit M, Dariane C, Verkarre V, Biard L, El Zein R, Lesaffre C, Galy-Fauroux I, *et al*: Multiplexed immunofluorescence analysis and quantification of intratumoral PD-1+ Tim-3+ CD8+ T Cells. J Vis Exp 132: 56606, 2018.
33. Liu T, Sun L, Zhang Y, Wang Y and Zheng J: Imbalanced GSH/ROS and sequential cell death. J Biochemical Mol Toxicol 36: e22942, 2022.
34. Hayashi H, Yasufuku I, Higashi T, Chikaishi W, Yokoi R, Fukada M, Sato Y, Asai R, Tajima JY, Saigo C, *et al*: Late recurrent gastric carcinoma 12 years after surgery with attenuation of CD44 variant 9 expression. Surg Case Rep 9: 87, 2023.
35. Ishimoto T, Nagano O, Yae T, Tamada M, Motohara T, Oshima H, Oshima M, Ikeda T, Asaba R, Yagi H, *et al*: CD44 variant regulates redox status in cancer cells by stabilizing the xCT subunit of system xc(-) and thereby promotes tumor growth. Cancer Cell 19: 387-400, 2011.
36. Bertaux-Skeirik N, Wunderlich M, Teal E, Chakrabarti J, Biesiada J, Mahe M, Sundaram N, Gabre J, Hawkins J, Jian G, *et al*: CD44 variant isoform 9 emerges in response to injury and contributes to the regeneration of the gastric epithelium. J Pathol 242: 463-475, 2017.
37. Jang BI, Li Y, Graham DY and Cen P: The role of CD44 in the pathogenesis, diagnosis, and therapy of gastric cancer. Gut and Liver 5: 397-405, 2011.
38. Engevik AC, Feng R, Choi E, White S, Bertaux-Skeirik N, Li J, Mahe MM, Aihara E, Yang L, DiPasquale B, *et al*: The development of spasmolytic polypeptide/TFF2-expressing metaplasia (SPEM) during gastric repair is absent in the aged stomach. Cell Mol Gastroenterol Hepatol 2: 605-624, 2016.
39. Topham DJ and Reilly EC: Tissue-resident memory CD8+ T cells: From phenotype to function. Front Immunol 9: 515, 2018.
40. Yi P, Cao P, Yang M, Xiong F, Jiang J, Mei Y, Xin Y, Zhao M, Wu H and Lu Q: Overexpressed CD44 is associated with B-cell activation via the HA-CD44-AIM2 pathway in lupus B cells. Clin Immunol 255: 109710, 2023.
41. Zhang Q, Wang X, Liu Y, Xu H and Ye C: Pan-cancer and single-cell analyses identify CD44 as an immunotherapy response predictor and regulating macrophage polarization and tumor progression in colorectal cancer. Front Oncol 14: 1380821, 2024.
42. Van Driel M, Günthert U, van Kessel AC, Joling P, Stauder R, Lokhorst HM and Bloem AC: CD44 variant isoforms are involved in plasma cell adhesion to bone marrow stromal cells. Leukemia 16: 135-143, 2002.
43. Johnson DE, O'Keefe RA and Grandis JR: Targeting the IL-6/JAK/STAT3 signalling axis in cancer. Nat Rev Clin Oncol 15: 234-248, 2018.
44. Fricke H, Hartmann J, Sitter T, Steldinger R, Rieber P and Schiffl H: Continuous ambulatory peritoneal dialysis impairs T lymphocyte selection in the peritoneum. Kidney Int 49: 1386-1395, 1996.
45. Cheung EC and Vousden KH: The role of ROS in tumour development and progression. Nat Rev Cancer 22: 280-297, 2022.
46. Pieters M, Kruger IM, Kruger HS, Breet Y, Moss SJ, van Oort A, Bester P and Ricci C: Strategies of modelling incident outcomes using cox regression to estimate the population attributable risk. Int J Environ Res Public Health 20: 6417, 2023.
47. Sauerbrei W, Perperoglou A, Schmid M, Abrahamowicz M, Becher H, Binder H, Dunkler D, Harrell FE Jr, Royston P and Heinze G: State of the art in selection of variables and functional forms in multivariable analysis-outstanding issues. Diagn Progn Res 4: 3, 2020.
48. Zhu N, Zhao Y, Yan W, Wei L, Sang Q, Li J, Liu B and Yu B: Characterization of alternative splicing events and prognostic signatures in gastric cancer. Cancer Cell Int 24: 167, 2024.
49. Cao M, Hu C, Pan S, Zhang Y, Yu P, Zhang R, Cheng X and Xu Z: Development and validation of nomogram for predicting early recurrence after radical gastrectomy of gastric cancer. World J Surg Oncol 22: 21, 2024.
50. Cai H, Li M, Deng R, Wang M and Shi Y: Advances in molecular biomarkers research and clinical application progress for gastric cancer immunotherapy. Biomark Res 10: 67, 2022.
51. Yang X, Li M, Qin X, Tan S, Du L, Ma C and Li M: Photophosphatidylserine guides natural killer cell photoimmunotherapy via TIM-3. J Am Chem Soc 144: 3863-3874, 2022.
52. Jiang J, Jin MS, Kong F, Cao D, Ma HX, Jia Z, Wang YP, Suo J and Cao X: Decreased galectin-9 and increased Tim-3 expression are related to poor prognosis in gastric cancer. PLoS One 8: e81799, 2013.
53. Zhou Y, Li S, Hu Y, Xu X, Cui J, Li S, Li Z, Ji J and Xing R: Multi-regional sequencing reveals the genetic and immune heterogeneity of non-cancerous tissues in gastric cancer. J Pathol 263: 454-465, 2024.
54. Wang YK, Lv XX, Wang ZQ, Zhou YM, Jiang B, Wang SN and Chen XD: The significance of the microlymphangiogenesis, microangiogenesis, and combined detection of programmed cell death-1 protein (PD-1)/ki67 in gastric cancer tissues. J Cancer Res Clin Oncol 149: 9129-9137, 2023.
55. Li L, Wu W, Zheng W, Hui Q and Zhao C: Analysis of the correlation between p27 expression and helicobacter pylori infection in gastric cancer. APMIS 130: 21-25, 2022.
56. Awadh M, Darwish A, Alqatari H, Buzaid FM and Darwish A: A descriptive analysis of gastric cancer with an immunohistochemical study of ki67 and p53 as prognostic factors.: Bahrain experience. Saudi Med J 44: 1300-1309, 2023.
57. Chen L, Hong J, Hu R, Yu X, Chen X, Zheng S, Qin Y, Zhou X, Wang Y, Zheng L, *et al*: Clinical value of combined detection of serum sTim-3 and pepsinogen for gastric cancer diagnosis. Cancer Manag Res 13: 7759-7769, 2021.
58. Wang H, Jin W, Wan C and Zhu C: Diagnostic value of combined detection of CA72-4, CA19-9, and carcinoembryonic antigen comparing to CA72-4 alone in gastric cancer: A systematic review and meta-analysis. Transl Cancer Res 11: 848-856, 2022.